UNIVERSITY OF BIRMINGHAM

Research at Birmingham

Phase diagram of germanium telluride encapsulated in carbon nanotubes from first-principles searches

Wynn, Jamie; Medeiros, Paolo; Vasylenko, Andrij; Sloan, Jeremy; Quigley, David; Morris, Andrew

Document Version
Peer reviewed version

Link to publication on Research at Birmingham portal

Phase diagram of germanium telluride encapsulated in carbon nanotubes from first-principles searches

Jamie M. Wynn,[1, *] Paulo V. C. Medeiros,[1] Andrij Vasylenko,[2, 3]
Jeremy Sloan,[2] David Quigley,[2] and Andrew J. Morris[1, 2, 4, †]

[1] *Theory of Condensed Matter Group, Cavendish Laboratory,*
University of Cambridge, Cambridge CB3 0HE, U.K.
[2] *Department of Physics, University of Warwick, Coventry CV4 7AL, U.K.*
[3] *Institute for Condensed Matter Physics, NAS of Ukraine, Lviv 79011, Ukraine*
[4] *School of Metallurgy and Materials, University of Birmingham, Edgbaston, Birmingham, B15 2TT, U.K.*
(Dated: December 13, 2017)

Germanium telluride has attracted great research interest, primarily due to its phase-change properties. We have developed a general scheme, based on the *ab initio* random structure searching (AIRSS) method, for predicting the structures of encapsulated nanowires, and using this we predict a number of novel thermodynamically stable structures of GeTe nanowires encapsulated inside carbon nanotubes of radii under 9 Å. We construct the phase diagram of encapsulated GeTe, which provides quantitative predictions about the energetic favourability of different filling structures as a function of the nanotube radius, such as the formation of a quasi-1D rocksalt-like phase inside nanotubes of radii between 5.4 and 7.9 Å. Simulated TEM images of our structures show excellent agreement between our results and experimental TEM imagery. We show that, for some nanotubes, the nanowires undergo temperature-induced phase transitions from one crystalline structure to another due to vibrational contributions to the free energy, which is a first step towards nano-phase change memory devices.

Germanium telluride is a chalcogenide whose phase-change properties make it the subject of considerable interest due to its non-volatile memory applications [1–5]. In particular, it undergoes a reversible, temperature-induced crystalline-amorphous transition in which the resistance of the amorphous phase is dramatically lower than that of the crystalline phase [6, 7]. These phase-change properties make GeTe a prime candidate for information storage technology [8] and have led to much research activity, both on GeTe itself and on related phase-change materials such as the ternary alloy GeSbTe (also known as GST) [9–11].

Low-dimensional forms of GeTe have also drawn significant attention, with thin films having been used in the recent past as rewritable optical disk memory [12], and GeTe nanoparticles having been investigated for their phase-change properties [13]. There has also been emerging interest in the technological potential of GeTe nanowires [14–18]. Experiments have found that, at least at larger radii, GeTe nanowires retain the bulk phase's technologically useful phase-switching properties[16, 19], and that their melting temperature is considerably lower than that of the bulk [20], hence they may be useful as phase-change components in low-power electronic devices.

Forcing a material to adopt a quasi-1D geometry only a few atoms wide significantly affects its behaviour and structure, as we show below (and can also modulate the behaviour of the encapsulating nanotube [21]). Therefore, to understand the behaviour of encapsulated GeTe, it must be studied in its own right, distinct from its bulk phase. However, despite experimental interest, encapsu-lated GeTe nanowires have received relatively little theoretical attention, possibly because of the modelling challenges involved.

To study the behaviour of encapsulated GeTe, we have adapted the *ab initio* random structure searching (AIRSS) method [22] for the prediction of encapsulated quasi-1D structures. We emphasise that less expensive structure prediction methods, such as data-mining crystal structure databases, are not applicable here since there are currently no such databases for quasi-1D structures. Thanks to its simplicity and flexibility, AIRSS has proven a powerful tool in the prediction of bulk structures [23–25] and defect complexes [26–28]; below, we present a systematic way to predict the structures formed by materials encapsulated inside nanotubes (and of quasi-1D systems in general).

From the results of the structure search we identify a range of novel, energetically favourable 1D crystalline structures and construct a phase diagram showing how the formation energy of each phase varies with the radius of the encapsulating single-walled nanotube (SWNT). We predict a series of phase transitions as different structures become the ground state with varying nanotube radius. We then calculate phonon free energies in order to explore the behaviour of encapsulated GeTe nanowires at finite temperature, and find the existence of several crystalline-crystalline temperature-induced phase transitions.

We use density-functional theory (DFT) as implemented in the CASTEP code [29] to compute energetics and to relax structures into minima of the potential energy landscape. The details of these calculations are given in the supporting information.

The underlying principle of AIRSS is to repeatedly generate physically reasonable initial structures and then relax them into local minima of the potential energy surface. While we retain this general scheme in adapting the AIRSS method to ENWs, some challenges arise. Firstly, even with cells of fairly short periodicity, a large number of carbon atoms must be included: for example, a 7.2 Å-long cell of the armchair (6,6) SWNT contains 72 carbon atoms. At the start of an AIRSS calculation one does not know *a priori* the periodic length of the relaxed structure, and the presence of the nanotube – which is highly resistant to longitudinal tension and compression – prevents the nanowire from optimising its periodicity during relaxation. This could introduce significant levels of strain in the encapsulated wire and thereby compromise the accuracy of the calculated energies. Moreover, to simulate this many atoms explicitly would make it difficult to attain the number of structures required to thoroughly sample the structure space. We solve these problems by replacing the carbon atoms with an external potential acting on the encapsulated material, which we justify by appealing to the chemical inertness of the SWNT itself. We choose the potential to take the form of a repulsive Gaussian function dependent only on distance from the central axis of the nanotube, peaking at the radius of the nanotube. The nanowire thus interacts with an 'implicit nanotube' which replicates the confining effects of the full nanotube at tiny fraction of the cost. The potential is discussed in more detail in the Supplemental Material [30].

To test the implicit nanotube approximation, we also performed some AIRSS searches (generating around 1100 structures) with explicit treatment of the SWNT. We found that *all* low-energy nanowire structures identified with full treatment of the SWNT were also found using the implicit nanotube, and surprisingly that some low-energy structures were *only* found using the implicit nanotube. This is because the inclusion of the nanotube means that only a discrete set of unit cell lengths is possible, and therefore only a subset of structure space is accessible to the search. The implicit nanotube approximation thus allows us to explore structure space not only more cheaply but also more thoroughly than if we had treated the carbon atoms fully within DFT. Previously, we have successfully used the implicit nanotube method to identify the structures of tellurium nanowires [31], which provides an experimental verification of the method's effectiveness.

Physically, one can anticipate (and our results confirm) that, for small nanotube radii, the structure of the nanowire will be determined primarily by the confining effect of the nanotube on the nanowire, resulting in close-packed structures. On the other hand, for large radii, the structure must become more bulk-like (since in the limit of large radii, the optimal structure must simply be a block of bulk GeTe in a very wide nanotube). We cap-

ture both of these extremes in our searches using a dual approach in which we generate some initial structures subject to the symmetry of a rod group – rod groups being the symmetry groups describing structures periodic in only one direction [32] – and some subject to the symmetry of a space group. In the first case, we select a random nanotube radius (from 3 to 9 Å) and a random unit cell length (of up to 14 Å) and insert Ge and Te atoms into the implicit nanotube subject to a randomly chosen rod group. We then relax the structure to an energetic minimum. In the second case, we select a random space group and randomly generate a bulk structure (*i.e.* one with 3D periodicity) subject to that space group. A cylindrical cut-through of this bulk structure is then made and is inserted into the implicit nanotube – once again of random radius – and, after ensuring that the stoichiometry of the filling is still 1:1 and stretching or compressing the filling to match the periodicity of the tube, we then optimise the structure. With both of these schemes combined, our AIRSS searches generated just over 6000 structures, with many ground-state structures being found dozens of times at each nanotube radius, which is an indication of the search's thorough coverage of structure space.

For each structure found in our AIRSS searches, we calculated the formation energy, which is given by

$$E_f = E_{\text{ENW}} - N_{\text{GeTe}}\mu_{\text{GeTe}} - N_{\text{C}}\mu_{\text{C}} - E_{\text{str}}(s), \quad (1)$$

where E_{ENW} is the DFT total energy of the encapsulated nanowire (ENW); N_{GeTe}, μ_{GeTe}, N_{C} and μ_{C} are the quantity and chemical potentials of a formula unit of GeTe and carbon atoms respectively; and $E_{\text{str}}(s)$ is a correction term to remove the strain energy due to mismatch between the periodicities of the nanowire and the nanotube. In the initial structure searches μ_{C} is zero because the C atoms have been replaced with an implicit nanotube, and there is also no strain energy term because, in the absence of the carbon atoms, we can allow the wire to relax to its equilibrium length.

After the AIRSS searches, we identified the lowest-energy structures at each nanotube radius (those with formation energies within around 0.1 eV per atom of the ground state) and re-relaxed each one in multiple nanotubes of differing radii, with carbon atoms treated fully within DFT rather than replaced with an implicit nanotube. For each nanowire structure, these calculations give the formation energy as a function of the radius of the encapsulating SWNT. The choice of which nanotubes – *i.e.* which chiral vector and repeat length – to insert the nanowires into was made based on the number of atoms in the nanotube and the resultant strain on the nanowire.

We always stretch (or compress) the wire to match the periodicity of the nanotube, rather than the other way around, since the nanowires are expected to be much less resistant to strain (*i.e.* less longitudinally rigid) than

nanotubes. To correct for the effects of the mismatch between the nanotube and the nanowire, we compute the energy cost of applying a strain s to the nanowire, $E_{str} = E(s) - E(0)$ (where $E(s)$ is the DFT total energy of the nanowire at a strain of s relative to its equilibrium length, and in the absence of the nanotube; $E(0)$ is then the energy in the absence of any applied strain, *i.e.* at the equilibrium length of the structure.). This is done for a range of values of the strain s, which we then interpolate to obtain the function $E_{str}(s)$. When computing the formation energies of ENWs, we use our interpolated value of E_{str} for the strain term in Eq. 1. In each case we use a geometry optimisation on the nanotube in question (absent any filling) to obtain μ_C. We use bulk GeTe as the source for the chemical potential μ_{GeTe}.

Having obtained the formation energy as a function of nanotube radius for the most stable nanowire structures, we plot them for each structure in figure 1. Each data point is the result of the full geometry optimisation of a supercell containing an explicitly simulated ENW. Table I summarises each phase's structure and symmetry.

Fig. 1 shows how wider structures tend to reach lower formation energies, since they tend to be more bulk-like. Every structure's formation energy follows the same trend of a rapid drop as the tube becomes wide enough to accommodate it, followed by a shallow minimum associated with a weak attraction between the nanowire and the nanotube, and eventually flattening out as the tube becomes so wide that its walls barely interact with the nanowire.

The shallowness of the minima in the formation energy curves confirms our previous assertion that the is no significant bonding between the nanotube and the wire. Additionally, across all of our ground-state nanowire structures, the closest distance between the nanotube and nanowire is a fairly large 3.28 Å between a Ge and C atom – 0.5 Å longer than a typical Ge-Te bond even though the Van der Waals radius of C is 0.4 Å less than that of Te. We also find no indication in the DFT charge densities of any tube-wire bonding.

The data showing the limit of the formation energy as the nanotube radius tends to infinity were computed by simulating the nanowire on its own, since as the nanotube radius tends to infinity the interaction between the nanowire and the nanotube walls must tend to zero. (This represents the asymptotic formation energy behaviour of a particular nanowire; however, experimentally one would expect to see a phase transition into a different, wider, nanowire structure as the nanotube radius increases.)

Note that it is to be expected that all the formation energies are positive, since we have chosen bulk GeTe as our reference for the chemical potential.

One can identify on fig. 1 a series of zero-temperature phase transitions as the radius grows and new structures become energetically favourable due to the greater size of the central cavity available to the nanowire. At very small radii, a series of Ge-Te dimers is formed, which the phase diagram shows is energetically preferable to the formation of a linear chain at all nanotube radii. At 3.7 Å the tube is wide enough that it becomes energetically favourable for a 1D chain of Ge and Te atoms to buckle into a zig-zag. At 4.8 Å, it becomes optimal to fit two of these zig-zags next to each other, increasing the coordination. Then, at 5.4 Å, a $2 \times 2 \times \infty$ cut-through of the rocksalt-like GeTe bulk forms. Beyond 8 Å a larger number of phases become energetically competitive, with the ground state passing through a series of increasingly wide rocksalt-like cut-throughs (after $P\bar{4}m2$, $Pcc2$ then $P\bar{4}mm$).

In ref. 33, Giusca *et. al* present a TEM image (reproduced here in fig. 2) of a 2×2 rocksalt-like phase of GeTe encapsulated within a nanotube of about 6 Å in radius. This is a good match to our phase diagram, which predicts that at this radius, the 2×2 rocksalt structure is the ground state. An image of a nanowire in a tube of radius around 5.5 Å also appears, containing a phase which the authors attribute to a rhombohedral structure. However, our results strongly suggest that this is in fact our $P\bar{1}$ double zig-zag structure (see table I), which at this nanotube radius we predict to be energetically competitive with 2×2 rocksalt. This illustrates the strength of combining theory and experiment in predicting crystal structures: the TEM data alone are not enough to uniquely identify the structure, but comparing the experimental data with our first-principles predictions allows us to do so with confidence. A comparison between this experimental imagery and some simulated TEM imagery based on our predicted structures is shown on figure 2, which shows that our predictions provide a close match with the TEM images.

The near-degeneracy of many of the phases, especially in wider nanotubes, suggests that at finite temperatures some of the metastable structures may become energetically competitive or even overtake the zero-temperature ground states in energetic favourability. To test this hypothesis, we performed harmonic phonon calculations to obtain the vibrational free energy of each phase as a function of temperature. These phonon calculations were performed within an implicit nanotube, and in each case the radius of the implicit nanotube was chosen to match that of the nanotube in which each structure was found to be most stable (relative to the other phases) on fig. 1.

Using the vibrational free energies along with the DFT total energies, we plot the most favourable nanowire structure as a function of nanotube radius and temperature on fig. 3. We did not find that finite temperature effects cause any phases which never form at zero temperature to become energetically favourable; however, we did find that the critical nanotube radii at which there are two degenerate ground state structures (shown as dashed vertical lines on fig. 1) are shifted noticeably as tempera-
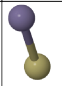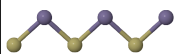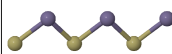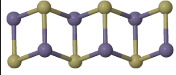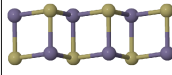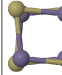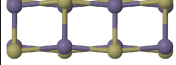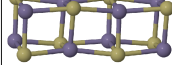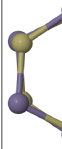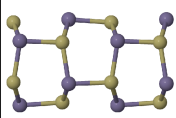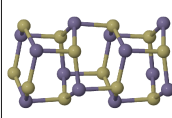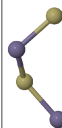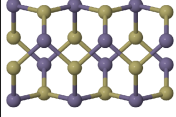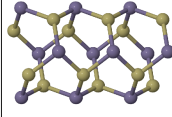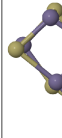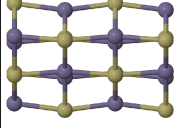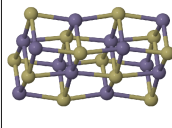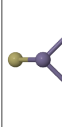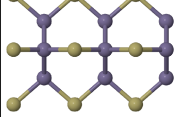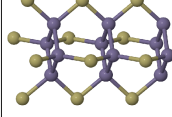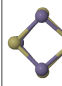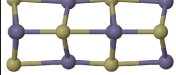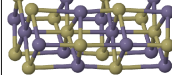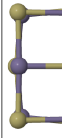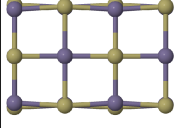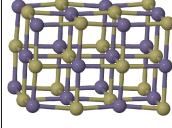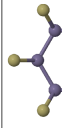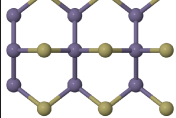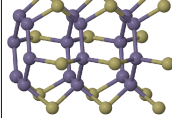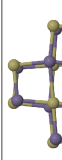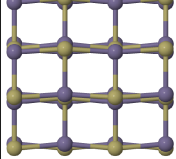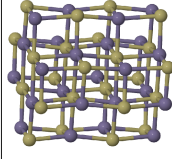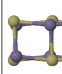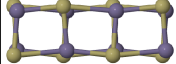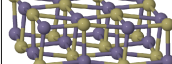
Structure	End-on view	Side-on view	3D view
$P\infty$ (1D dimers)			
$P\infty/m$ (1D chain)			
$Pm2m$ (Zig-zag)			
$P\bar{1}$ (Parallel zig-zag)			
$P\bar{4}m2$ (2x2 rocksalt)			
$P3mm$ (Diatomic rings)			
$P\bar{4}$ (Zincblende-like)			
$Pmm2$-I (2x3 rocksalt)			
$P4/mmm$-I (Monatomic rings)			
$Pmm2$-II (Truncated 3x3 rocksalt)			
$P4/mmm$-II (3x3 rocksalt)			
$P6/mmm$ (Monatomic rings)			
$P\bar{4}mm$ (Plus-shaped rocksalt)			
$Pcc2$ (2x4 rocksalt)			

TABLE I. All GeTe filling structures shown on figure 1. In the end-on view the periodic axis points into the page and in the side-on view it points from left to right. Where two structures have the same symmetry, we distinguish them by appending a number in Roman numerals.
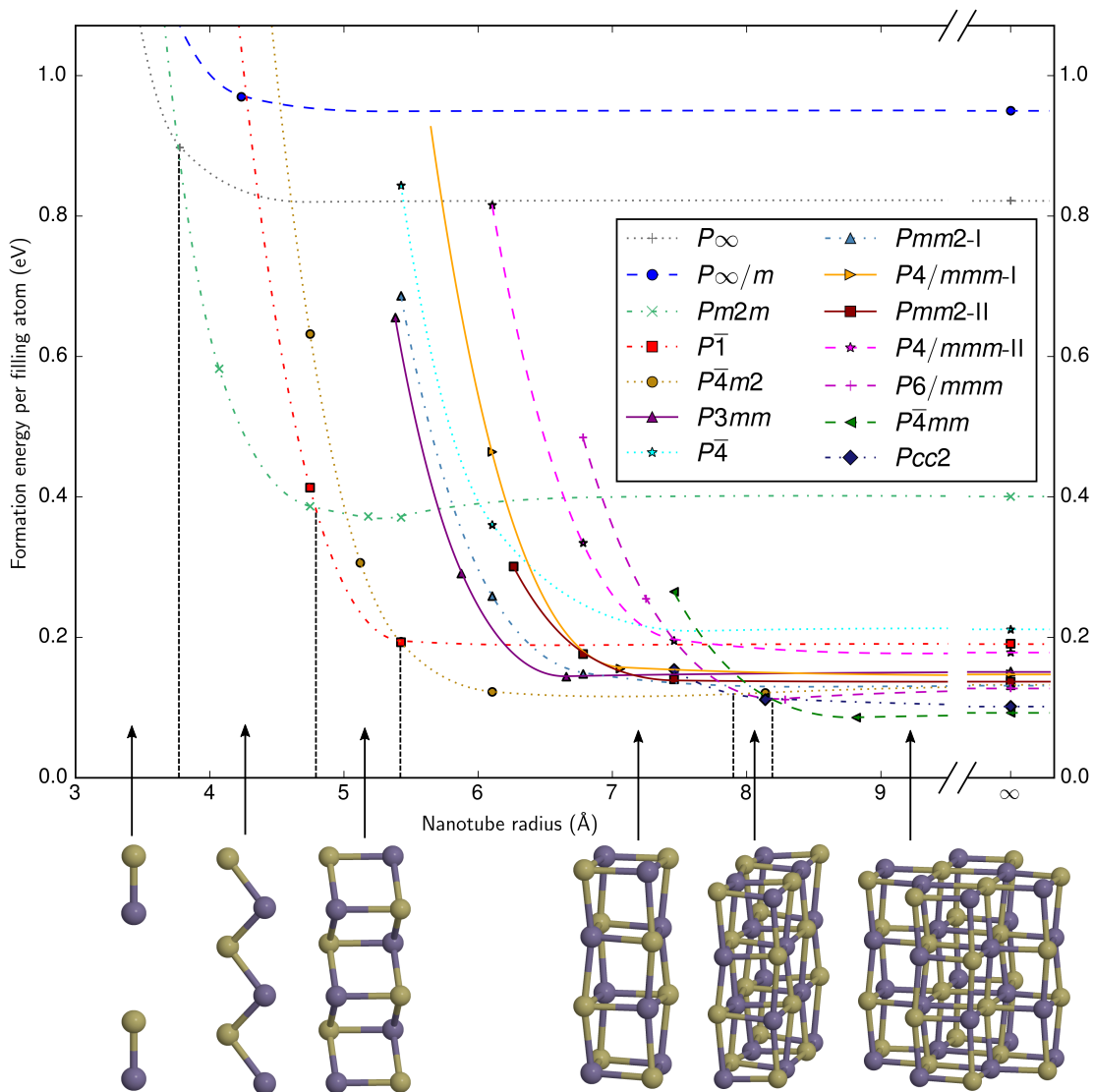
FIG. 1. Zero-temperature phase diagram for encapsulated GeTe nanowires. Where a line begins without a data point (e.g. as in the $P4/mmm-$I phase at 5.65 Å), the structure was found to be mechanically unstable in a nanotube of that radius. In this case the energy from that calculation is not included in the fit, and the fit is then extrapolated to that point. The vertical dotted black lines indicate the positions of phase transitions at which a new nanowire phase becomes the most energetically favourable. The ground state structures are shown along the bottom, with the arrows pointing to the regions on the phase diagram at which they are the most energetically favourable structures.

ture varies. An important consequence of this is that, for certain nanotube radii, heating up the ENW will induce a crystalline-crystalline phase transition. We have identified all sets of chiral vectors in which such a transition will occur. These are shown in table II. These crystalline-crystalline transitions appear to have no analogy in the bulk phase, and therefore suggest that GeTe behaves in a qualitatively different manner when strongly confined to one dimension.

In summary, we have investigated the formation of 1D crystals by GeTe encapsulated within carbon nanotubes using *ab initio* random structure searching (AIRSS). By computing their formation energy as a function of the ra-

dius of the encapsulating nanotubes we have constructed a phase diagram for encapsulated GeTe nanowires that quantitatively maps out a sequence of structures as progressively wider nanotubes are considered. Our results predict a range of novel phases which are often strikingly different from the bulk, and thereby shed light on the change in behaviour of GeTe when confined to atomically thin spaces. Our predictions run across a large range of nanotube radii, and where experimental imagery is available, we have matched it.

We have also found that the finite-temperature behaviour of GeTe ENWs contains a number of crystalline-crystalline temperature-induced phase transitions. The
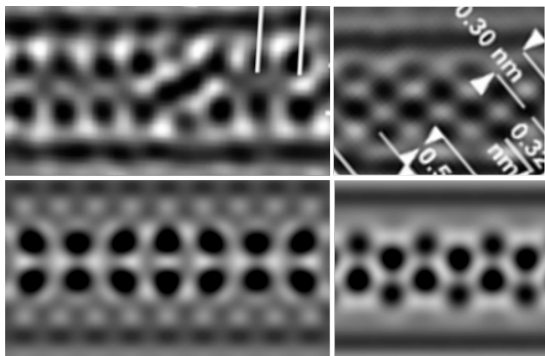
FIG. 2. A comparison between experimental TEM imagery reproduced with permission from ref. 33 (top) and simulated TEM imagery (bottom) generated from the GeTe structures predicted in this work using SimulaTEM's 'multislic' package [34]. The structures shown are the $P\bar{4}m2$ (left) and $P\bar{1}$ (right) phases.

Chiral vector	Radius (Å)	Structures	Temp. (K)
(9,5)	4.81	$P\bar{1}\rightarrow Pm2m$	310
(10,4)	4.89	$P\bar{1}\rightarrow Pm2m$	980
(12,3)	5.38	$P\bar{1}\rightarrow P\bar{4}m2$	630
(15,8)	7.92	$Pcc2\rightarrow P\bar{4}m2$	220
(18,4)	7.95	$Pcc2\rightarrow P\bar{4}m2$	460
(16,7)	8.00	$Pcc2\rightarrow P\bar{4}m2$	860
(18,5)	8.20	$P\bar{4}mm\rightarrow Pcc2$	130
(15,9)	8.22	$P\bar{4}mm\rightarrow Pcc2$	230
(21,0)	8.22	$P\bar{4}mm\rightarrow Pcc2$	230
(20,2)	8.25	$P\bar{4}mm\rightarrow Pcc2$	340
(16,8)	8.29	$P\bar{4}mm\rightarrow Pcc2$	510
(19,4)	8.33	$P\bar{4}mm\rightarrow Pcc2$	680
(17,7)	8.37	$P\bar{4}mm\rightarrow Pcc2$	790
(21,1)	8.42	$P\bar{4}mm\rightarrow Pcc2$	950

TABLE II. Nanotubes at which our finite-temperature calculations indicate the presence of a phase transition between 0 and 1000 K. In the 'structures' column, the lower-temperature phase is indicated on the left and the higher-temperature phase on the right.

presence of such phase transitions illustrates a key feature in the behaviour of encapsulated nanowire systems: because the formation energies of different phases are strongly dependent on the radius of the encapsulating nanotube, the choice of nanotubes in which to encapsulate the wire acts as a means of 'tuning' the relative energies of different phases, with corresponding effects on ground state structures and phase transition temperatures. In this sense, the nanotube radius plays an analogous role to that of pressure in a traditional phase diagram, by adjusting the extent to which more compact structures are energetically incentivised.

The fact that the phase diagram of encapsulated GeTe contains crystalline-crystalline phase transitions which do not correspond to any analogous behaviour in the

bulk phase suggests that encapsulated GeTe nanowires may have unique technological applications; in particular, the possibility of a temperature-induced phase transition whose transition temperature is tunable via the choice of the radius of the encapsulating nanotube may have technological potential in the context of phase-change memory.

In addition, while we have only applied our structure searching method to GeTe in this work, the method is sufficiently flexible as to be broadly applicable to encapsulated nanowires and other quasi-1D systems in general, representing a significant new frontier in first-principles structure prediction.

* jw870@cam.ac.uk
† a.j.morris.1@bham.ac.uk

[1] G. Bruns, P. Merkelbach, C. Schlockermann, M. Salinga, M. Wuttig, T. D. Happ, J. B. Philipp, and M. Kund, Appl. Phys. Lett. 95, 43108 (2009).

[2] P. Nukala, C.-C. Lin, R. Composto, and R. Agarwal, Nat. Commun. 7, 10482 (2016).

[3] W. W. Koelmans, A. Sebastian, V. P. Jonnalagadda, D. Krebs, L. Dellmann, and E. Eleftheriou, Nat. Commun. 6, 8181 (2015).

[4] J. Y. Raty, W. Zhang, J. Luckas, C. Chen, R. Mazzarello, C. Bichara, and M. Wuttig, Nat. Commun. 6, 7467 (2015).

[5] K. Shportko, S. Kremers, M. Woda, D. Lencer, J. Robertson, and M. Wuttig, Nat. Mater. 7, 653 (2008).

[6] A. H. Edwards, A. C. Pineda, P. A. Schultz, M. G. Martin, A. P. Thompson, H. P. Hjalmarson, and C. J. Umrigar, Phys. Rev. B 73, 45210 (2006).

[7] G. C. Sosso, G. Miceli, S. Caravati, J. Behler, and M. Bernasconi, Phys. Rev. B 85, 174103 (2012).

[8] J. Akola and R. O. Jones, Phys. Rev. B 76, 235201 (2007).

[9] J. Akola, R. O. Jones, S. Kohara, S. Kimura, K. Kobayashi, M. Takata, T. Matsunaga, R. Kojima, and N. Yamada, Phys. Rev. B 80, 020201 (2009).

[10] K. S. Andrikopoulos, S. N. Yannopoulos, A. V. Kolobov, P. Fons, and J. Tominaga, J. Phys. Chem. Solids 68, 1074 (2007).

[11] J. M. Skelton, A. R. Pallipurath, T. H. Lee, and S. R. Elliott, Adv. Funct. Mater. 24, 7291 (2014).

[12] M. Wuttig and N. Yamada, Nat. Mater. 6, 824 (2007).

[13] M. A. Caldwell, S. Raoux, R. Y. Wang, H.-S. Philip Wong, and D. J. Milliron, J. Mater. Chem. 20, 1285
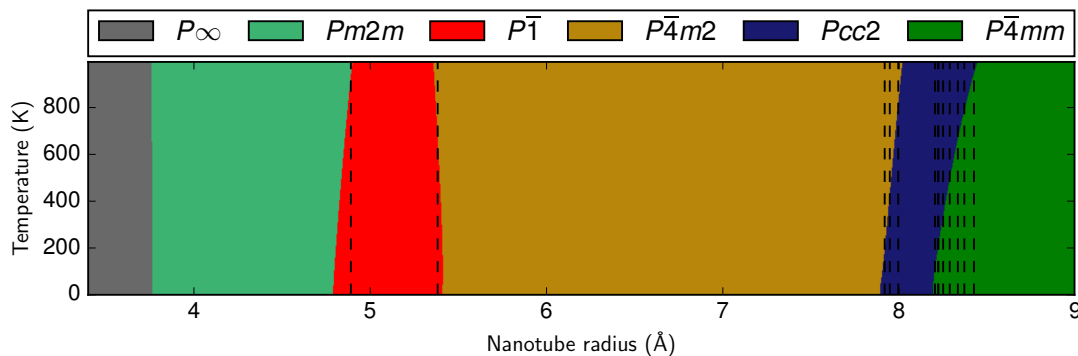
FIG. 3. The variation with nanotube radius and temperature of the ground-state nanowire structure. Variations in vibrational contributions to the structures' free energies are seen to induce changes in the nanotube radii at which transitions occur as the temperature varies, with the result that for certain nanotube radii, a temperature-induced phase transition is expected; these radii are marked with vertical dotted lines, and their corresponding chiral vectors are indicated in table II.

[14] P. Nukala, R. Agarwal, X. Qian, M. H. Jang, S. Dhara, K. Kumar, A. T. C. Johnson, J. Li, and R. Agarwal, Nano Lett. **14**, 2201 (2014).

[15] A. T. Jennings, Y. Jung, J. Engel, and R. Agarwal, J. Phys. Chem. C **113**, 6898 (2009).

[16] D. Yu, J. Wu, Q. Gu, and H. Park, J. Am. Chem. Soc. **128**, 8148 (2006).

[17] M.-K. Lee, T. G. Kim, B.-K. Ju, and Y.-M. Sung, Cryst. Growth Des. **9**, 938 (2009).

[18] J. W. L. Yim, B. Xiang, and J. Wu, J. Am. Chem. Soc. **131**, 14526 (2009).

[19] D. Yu, J. Wu, Q. Gu, and H. Park, J. Am. Chem. Soc. **128**, 8148 (2006).

[20] X. Sun, B. Yu, G. Ng, and M. Meyyappan, J. Phys. Chem. C **111**, 2421 (2007).

[21] A. Vasylenko, J. Wynn, P. V. Medeiros, A. J. Morris, J. Sloan, and D. Quigley, Phys. Rev. B **95**, 121408 (2017).

[22] C. J. Pickard and R. J. Needs, J. Phys. Condens. Matter **23**, 53201 (2011).

[23] C. J. Pickard and R. J. Needs, Nat Mater **9**, 624 (2010).

[24] J. M. Stratford, M. Mayo, P. K. Allan, O. Pecher, O. J. Borkiewicz, K. M. Wiaderek, K. W. Chapman, C. J. Pickard, A. J. Morris, and C. P. Grey, J. Am. Chem. Soc. **139**, jacs.7b01398 (2017).

[25] C. George, A. J. Morris, M. H. Modarres, and M. De Volder, Chem. Mater. **28**, 7304 (2016).

[26] J. Mulroue, A. J. Morris, and D. M. Duffy, Phys. Rev. B **84**, 094118 (2011).

[27] A. J. Morris, C. P. Grey, R. J. Needs, and C. J. Pickard, Phys. Rev. B **84**, 224106 (2011).

[28] A. J. Morris, C. J. Pickard, and R. J. Needs, Phys. Rev. B **80**, 144112 (2009).

[29] S. J. Clark, M. D. Segall, C. J. Pickard, P. J. Hasnip, M. I. J. Probert, K. Refson, and M. C. Payne, Zeitschrift fur Krist. **220**, 567 (2005).

[30] See Supplemental Material at [URL will be inserted by publisher] for technical information on the DFT calculations performed in this work and discussion of the form of the confining potential.

[31] P. V. Medeiros, S. Marks, J. M. Wynn, A. Vasylenko, Q. M. Ramasse, D. Quigley, J. Sloan, and A. J. Morris, ACS Nano **11**, 6178 (2017).

[32] V. Kopský and D. B. Litvin, eds., International Tables for Crystallography, Vol. E, 2nd online ed., Vol. E (International Union of Crystallography, Chester, England, 2010) pp. 290–291.

[33] C. E. Giusca, V. Stolojan, J. Sloan, F. Börrnert, H. Shiozawa, K. Sader, M. H. Rümmeli, B. Büchner, S. R. P. Silva, F. Bo Rrnert, H. Shiozawa, K. Sader, M. H. Ru Mmeli, B. Bu, S. Ravi, and P. Silva, Nano Lett. **13**, 4020 (2013).

[34] A. Gómez-Rodríguez, L. M. Beltrán-del Río, and R. Herrera-Becerra, Ultramicroscopy **110**, 95 (2010).